CHAPTER IV
RESULTS AND DISCUSSION

4.1 Synthesis of KL Zeolites by Microwave Heating Technique

According to Verduijn (1991 and 1995) potassium zeolites of type L (L zeolite) in which the crystals are very flat cylinders of "hockeypuck" were prepared by adding small amount of barium into synthesis mixture. The formula of synthesis mixture was 2.65 K_2O/0.0032 BaO/0.5 Al_2O_3/10 SiO_2/159 H_2O with barium concentration of 115 ppm. The synthesis mixture was heated by hot air (conventional method) at temperature of 443 K for 96 hours. The resulting zeolite was particularly useful as a base for aromatization catalysis by loading Pt. The process have a good yield and selectivity for desired reforming products and the catalyst is stable, is associated with low rate of coke formation, and has a long catalytically active life before regeneration required. In this study, therefore, elevated temperature of 443 K and such ratio of the synthesis mixture were selected for KL zeolite synthesis by MW. Because of the difference in the heating source between this work and Verduijn's work, the optimum synthesis conditions should be determined.

4.1.1 Optimum Ageing Time and Crystallization Time

To obtain the KL zeolite with high crystallinity, the optimum synthesis conditions were determined by varying ageing time and crystallization time. A series of synthesized products obtained were tabulated in Table 4.1.

The products were subsequently analyzed by XRD measurements. Representatives of XRD patterns are shown in Figures 4.1 and 4.2. From XRD data, phase of products can be identified as summarized in Table 4.1 and shown in Figure 4.3. Crystallinity percentage of all samples, additional results from XRD data, could be calculated by comparing against that of commercial KL zeolite (considered as having 100% crystallinity). These values are also presented in Table 4.1.

Separate tests were conducted using SEM technique examine the morphology and crystal size of the synthesized KL zeolites. A few samples with

high crystallinity as indicated by XRD technique were selected for SEM measurements. Figures 4.4 and 4.5 show SEM photographs of these samples. As shown in Figure 4.4, the morphology of the crystal was in a cylindrical shape with the crystal size ranging from 1 to 2 microns. The phase transformation was observed that amorphous phase would be reduced with an increasing crystallization time from 25 to 30 hr. This corresponds to the XRD results. Therefore, SEM results can confirm the validity of crystallinity percentage evaluated by XRD.

Table 4.1 Crystallinity percentage and phase of the synthesized products

Product name	Crystallinity (%)	Phase of product		Product name	Crystallinity (%)	Phase of product
A0/C30	50.9	A+C		A17/C25	62.6	A+KL
A0/C40	31.8	A		A17/C30	82.2	KL
A0/C50	53.5	KL+C		A17/C35	58	KL+C
A5/C30	37.8	A+KL+C		A24/C25	17	KL+A
A5/C40	54.1	C		A24/C30	105.6	KL
A5/C50	40.1	KL+C		A24/C37	77.9	KL
				A24/C41	26	KL+C
A15/C25	57.6	A+KL		A30/C25	9.3	A
A15/C30	62.4	A+KL		A30/C30	54.6	A+KL
A15/C40	65	KL+C		A30/C40	16.5	A+KL
A15/C50	29	C		A30/C45	16.6	KL+C

Note: A0/C30 represents 0 hr ageing time, 30 hr crystallization time. A, K and C represent amorphous, KL zeolite and other crystal phase, respectively. The crystallinity percentage of commercial KL zeolite is 100.
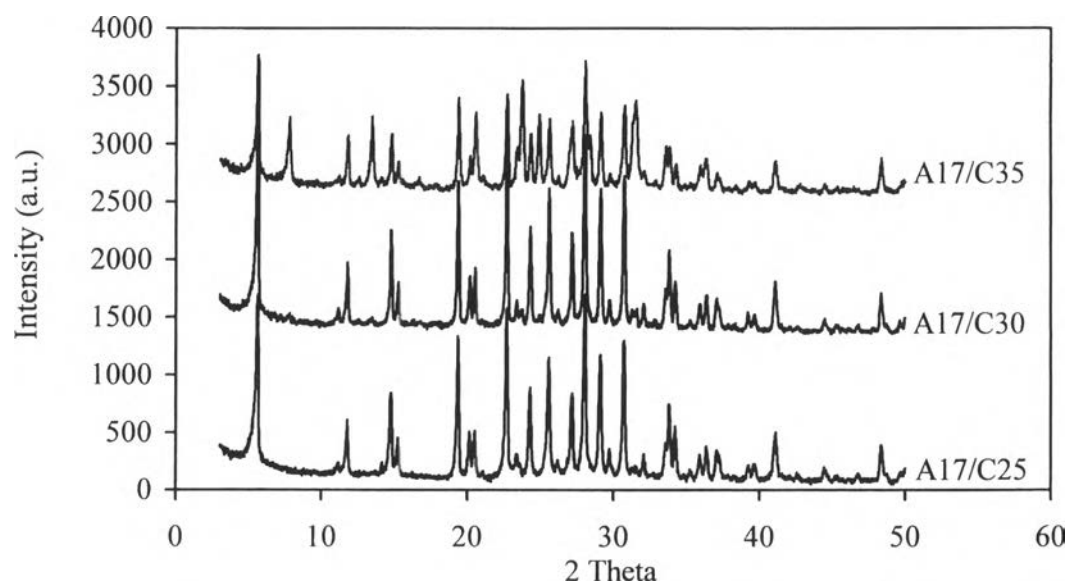
Figure 4.1   XRD patterns of synthesized KL zeolite obtained with different crystallization times at crystallization temperature of 443 K and ageing time of 17 hr.
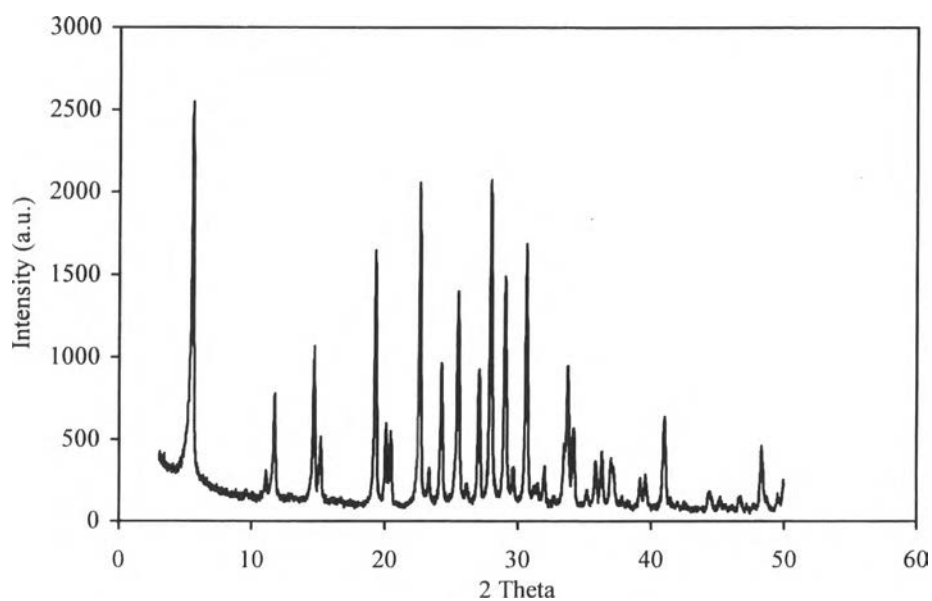

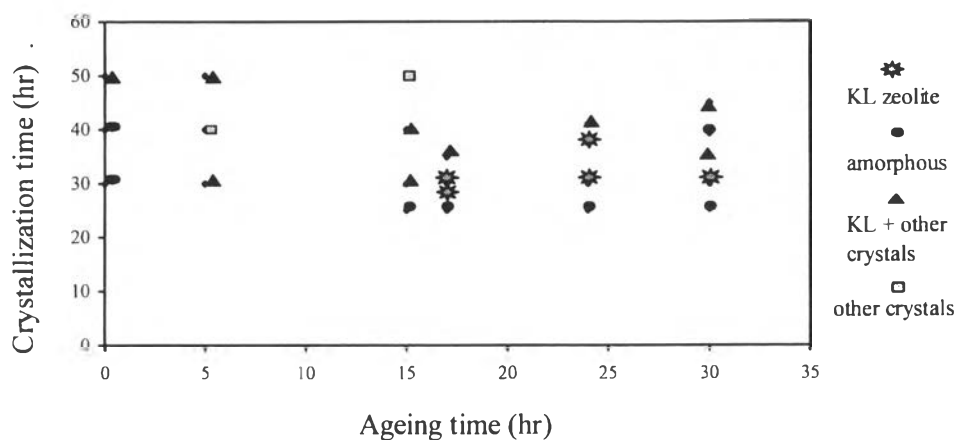**Figure 4.2** XRD pattern of commercial KL zeolite.

Figure 4.3 Product phase transformed at various crystallization times and ageing times.
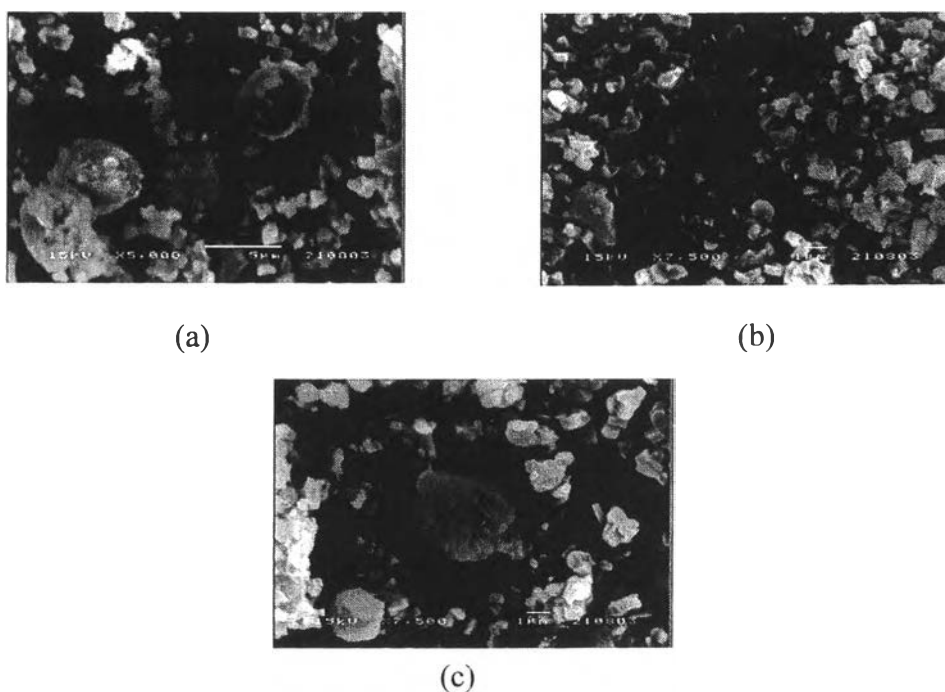

(a)   (b)

(c)

Figure 4.4 SEM photographs of synthesized KL zeolite crystals obtained with (a) crystallization time 20 hr (A17/C20), (b) 25 hr (A17/C25), and (c) 30 hr (A17/C30) at ageing time of 17 hr and crystallization temperature of 443 K.
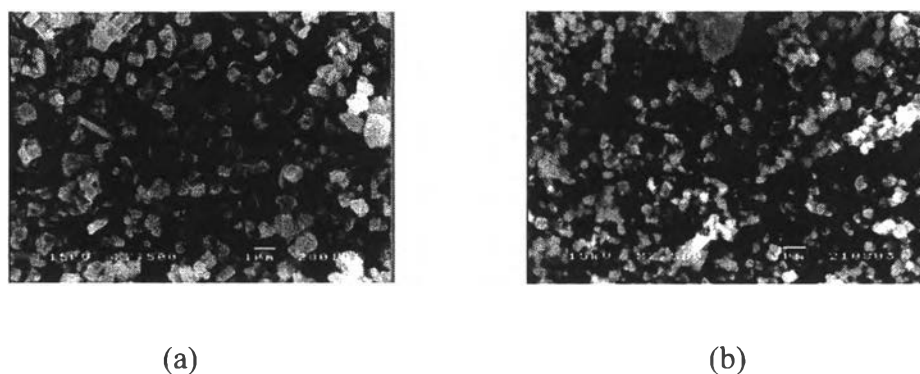
(a)   (b)

Figure 4.5 SEM photographs of synthesized KL zeolite crystals obtained with (a) ageing time of 30 hr and crystallization time of 30 hr (A30/C30) and (b) commercial KL zeolite.

According to XRD and SEM measurements of Figure 4.1, A17/C30 provided a high crystallinity without cocrystallization but A17/C35 gave contradictory results. In addition, A17/C25 showed a lower crystallinity than A17/C30. It can be explained that at 17 hours of the ageing time with low crystallization time such as 25 hours, complete growth of the crystal was not yet achieved. In contrast, 30 hours was sufficient for complete crystal growth. However, prolonged heating of as long as 35 hours resulted in dissolution and regrowth of the different crystals (Ertl, 1997).

As shown in Table 4.1 and Figure 4.3, the heating time and ageing time resulting in the KL zeolite products with less amount of other crystals and amorphous phase are in the range of 27-37 hours and above 17 hours, respectively. Therefore, the optimum ageing time and crystallization time were within this region. The short crystallization time of 27-37 hours was a result of microwave irradiation as it provided a higher heating rate, faster dissolution of gel, and more homogeneous heating when compared with 96 hours by conventional heating process (Verduijn, 1991, Bonaccorsi, 2003, Garcia, 1997, Girnus, 1995, Kodaira,1999, Pilter, 2000, and Xu, 2001).

Moreover, a low crystallinity percentage at the ageing time of less than 17 hours as shown in Figure 4.6 can be explained by an insufficient amount of nuclei in

the mixture. During KL zeolite preparation, gel solid started to form after mixing potassium aluminate solution to colloidal silica. Subsequently, the gel solid was dissolved by hydroxide ion to form small particles which condensed into nuclei. By the application of heat, the nuclei grew into crystal. This nuclei formation process took a certain period of time to complete. However, amount of nuclei decreased from ageing time of 24 to 30 hours because some of them was dissolved into monomer resulting in low crystallinity percentage (Ertl, 1997).

Hence, the ageing time of less than 17 hours is considered inadequate resulting in a low crystallinity percentage and nonhomogeneous synthesis mixture. To obtain a homogeneous synthesis mixture with a high crystallinity percentage, the ageing time at least 17 hours is required. Therefore, ageing of synthesis mixture of KL zeolite is a pre-step before the heating step. Contrasting conventional synthesis, the mixing and formation of nuclei can take place during the slow heat-up. So ageing step of KL zeolite is not necessary for a successful synthesis (Slangen, 1996).
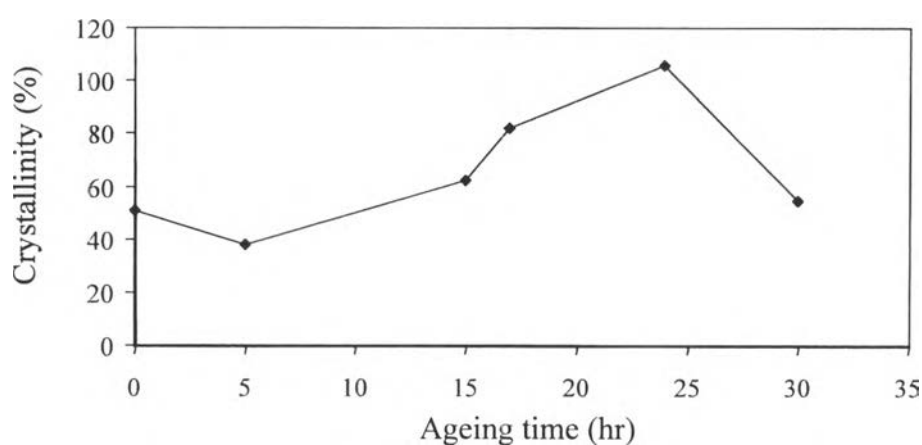
Figure 4.6 Crystallinity percentage at various ageing times at crystallization temperature of 443 K and crystallization time of 30 hours.

As mentioned before, the main objective of this work was to investigate the effect of crystal size on the product distribution. According to several publications (Kodaira,1999, Ertl, 1997, Slangen, 1996, and Xu, 2001), It was found that increase of ageing time resulted in decrease of crystal size of zeolite. Moreover, as described by Verduijn (1987) small amount of barium acted as nuclei or seed in KL zeolite synthesis. Therefore, variation of ageing time and barium concentration were conducted to obtain different crystal sizes of KL zeolite during the synthesis process.

4.1.2 The Impact of Ageing Time on Crystal Size

Table 4.2 summarizes the physical properties of synthesized KL zeolites in terms of thermal stability, crystallinity percentage, surface area, pore volume and crystal size. The crystal size was dramatically reduced when the gel was aged between 17 and 24 hours at crystallization time of 30 hours. It is possible that ageing of the gel enhanced the concentration of precursor species and the concentration of nuclei. Therefore, the average final crystal size was reduced when a larger number of nuclei developed into crystals. However, the ageing time of 30 hours gave a larger crystal size and low crystallinity percentage. This result indicated that amounts of nuclei were decreased at high ageing time when some precursors and nuclei would be dissolved into monomer (Ertl, 1997).

4.1.3 The Impact of Barium Concentration on Crystal Size

As summarized in Table 4.3, it was observed that an increase in crystal size resulted from an increasing amount of barium. The function of the added barium is not completely understood. But at least some of barium are believed to form very fine suspended silicate particles which will function as nuclei or seeds for KL zeolite formation (Verduijn, 1987). However, barium was observed to act as impurity that might retard the nuclei formation when its concentration reached 230 ppm. The crystal sizes of different barium concentrations are also shown in Figure 4.7. The A24/C30/B3 crystal size with higher amounts of barium was larger than that of A24/C30/B2 with lower amounts of barium. Moreover, it was also observed

that the crystallinity percentage of the synthesized products is somewhat constant but higher than that of the commercial zeolite.

Table 4.2 Physical properties of synthesized KL zeolites with various ageing times at crystallization time of 30 hr and commercial KL zeolite

Product name	Crystal size (micron)	Crystallinity (%)	Thermal stability (K)	Si/Al ratio	Surface area (m²/g)	Pore volume (cc/g)
A17/C30	1.74	82.21	>1073	3.55	124	0.092
A24/C30	1.35	105.59	>1073	3.28	144	0.093
A30/C30	2.19	54.61	>1073	n/a	n/a	n/a
comKL	0.65	100.00	>1073	3.02	277	0.243

Note: comKL represents commercial KL zeolite.

Table 4.3 Physical properties of synthesized KL zeolites with various amounts of barium added at crystallization time of 30 hr and commercial KL zeolite

Product name	Crystal size (micron)	Crystallinity (%)	Thermal stability (K)	Si/Al ratio	Surface area (m²/g)	Pore volume (cc/g)
A24/C30	1.35	105.59	>1073	3.28	144	0.093
A24/C30/B2	1.63	105.41	>1073	n/a	147	0.122
A30/C30/B3	2.07	105.41	>1073	3.27	156	0.121
comKL	0.65	100.00	>1073	3.02	277	0.243

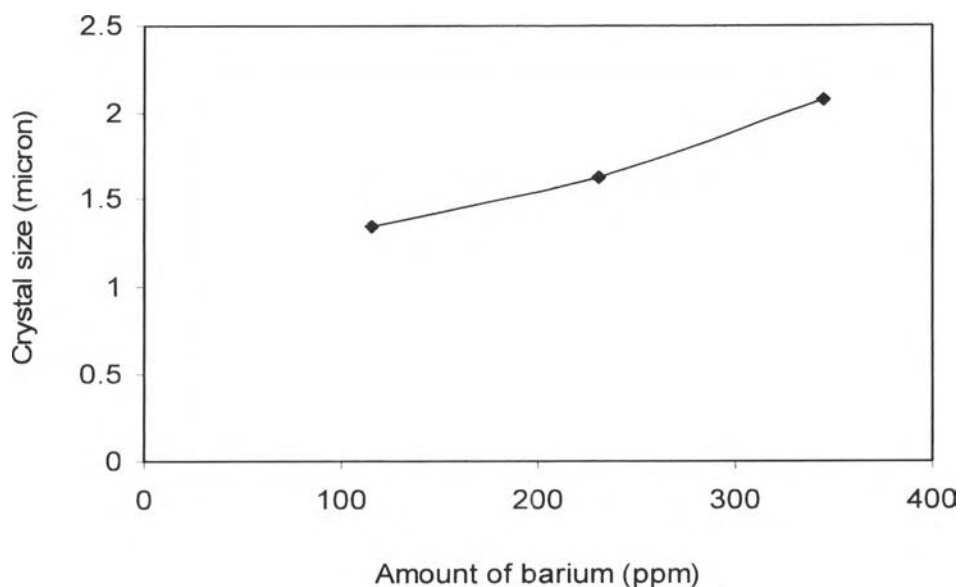Note: B2 and B3 represent 230 and 345 ppm barium amount added, respectively.

Figure 4.7 Crystal size with various amounts of barium at crystallization time of 30 hours, ageing time of 24 hours and crystallization temperature of 443 K.

Due to high crystallinity of A17/C30, A24/C30, and A24/C30/B3 with different cystal sizes, these products were selected for further characterization and the reaction tests.

4.2 Characterization of Synthesized KL Zeolites

Surface area, Si/Al ratio, and thermal stability of the synthesized and commercial KL zeolites are given in Table 4.2 and 4.3   Thermal stability of KL zeolites obtained were evaluated using a TG/DTA system in the temperature range of 298 to 1073 K. All samples gave the same thermal stability results. For example, TGA thermogram of A24/C30 as shown in Figure 4.8 revealed on the endothermic weight loss at 393 K which is the characteristic of KL zeolite. The weight loss corresponded to desorption/dehydration of physically sorbed or occluded water. TGA did not indicate any high temperature exotherm characteristics of lattice breakdown at least up to 1073 K. This indicates that A24/C30 is structural stability at least up to 1073 K (Yon sig ko,1998).
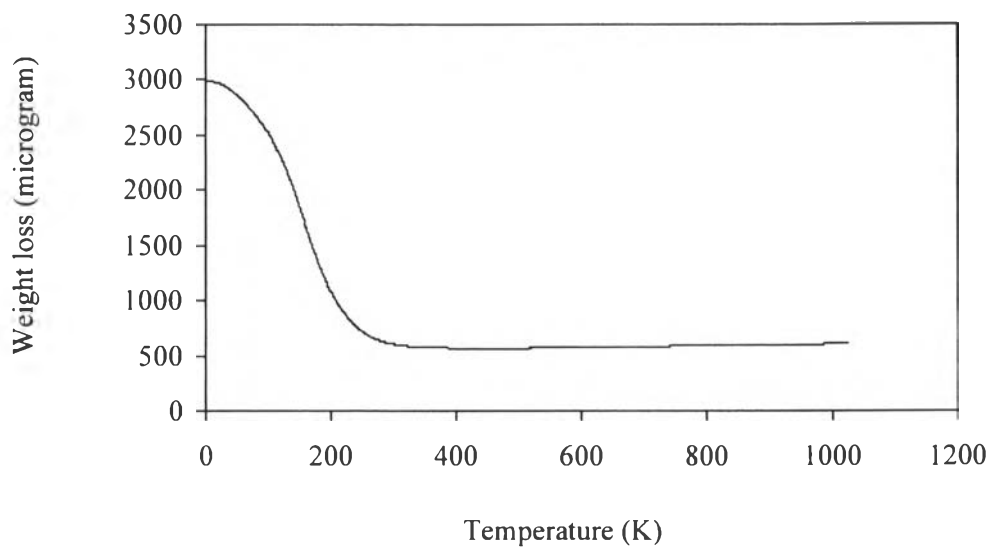
Figure 4.8 TGA thermogram of A24/C30.

4.3 Characterization of the Catalysts

1 % of Pt was loaded on synthesized KL zeolites by vapour phase impregnation method. After that the amount, dispersion percentage, and location of Pt on synthesized KL zeolites were determined by atomic absorption spectroscopy, hydrogen chemisorption, and FTIR of adsorbed CO, respectively.

4.3.1 Atomic Absorption Spectroscopy

This technique is used for finding the amount of Pt on synthesized KL zeolites. % Pt loading of all the samples were similar and nearly 1 (see Table 4.4).

Table 4.4 Amount of platinum loading and platinum dispersion of the catalysts prepared

Item	Catalyst name			
	Pt/A24/C30	Pt/A17/C30	Pt/A24/C30/B3	Pt/comKL
Pt loading (%)	0.94	0.96	0.94	1.03
H_2 chemisorption (%)	83.78	108.12	132.2	82.56

4.3.2 Hydrogen Chemisorption

The aim of conducting hydrogen chemisorption experiments was to obtain information on the dispersion of Pt clusters. As shown in Table 4.4, All of samples gave hydrogen chemisorption in the range of 82.00-132.20 %. These values indicate that Pt clusters were well dispersed on support surface and that almost all active sites were exposed to the reactant.

4.3.3 Diffuse Reflectance Infared Fourier Transform Spectrocopy (DRIFTS) of Adsorbed CO

FTIR of adsorbed CO has been widely used to characterize Pt/KL catalysts. In most FTIR measurements of CO adsorption on Pt/KL a series of the bands between 2080 and 1950 cm^{-1} have been observed. The bands of low wavenumber below 2075 cm^{-1} are related to the Pt clusters located inside the channels of the L zeolite while the bands at and above 2075 cm^{-1} are due to Pt external to the pores (Jacobs, 1999 and 2001). The spectra of Pt/A17/C30, Pt/A24/C30, Pt/A24/C30/B3, and Pt/commercial KL zeolite are shown in Figure 4.9. These results inferred that all of catalysts gave a similar shape of spectra having most of Pt clusters inside the channel. Moreover, the bands at different wave numbers are often used to identify the degrees of metal-zeolite interaction. Distribution of bands at lower wavenumbers reflects the higher degrees of metal-zeolite interaction and the smaller size of Pt clusters (Jacobs, 1999). For example, Pt/A24/C30/B3 showed FTIR bands at the lowest wave number and gave the highest hydrogen chemisorption resulting in highest degree of metal-zeolite interaction.
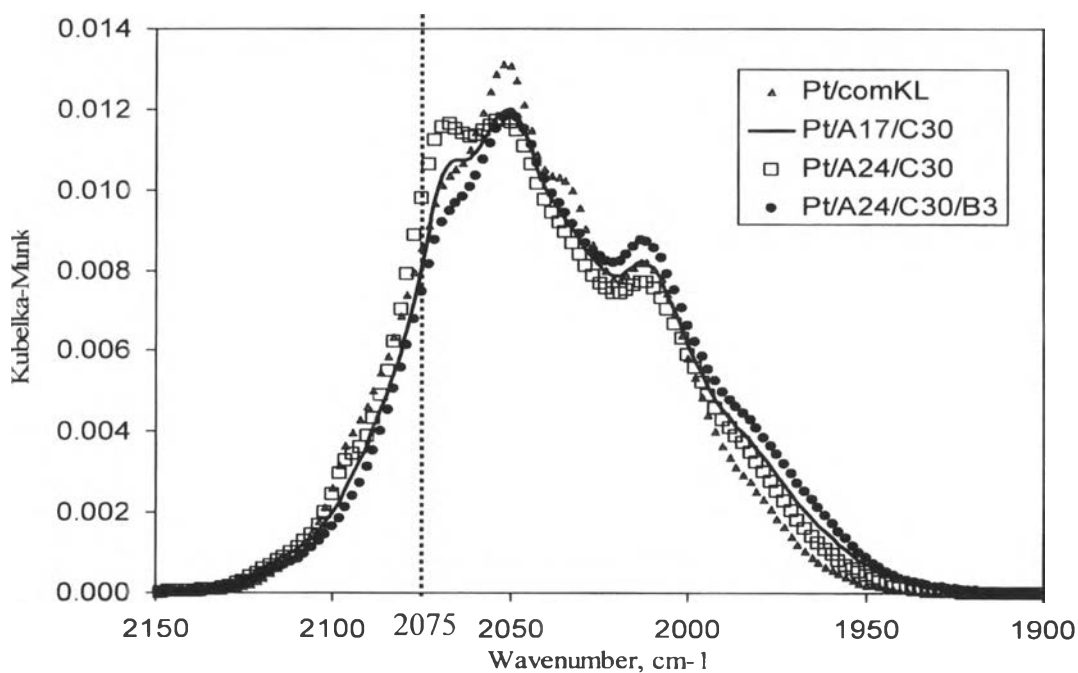
Figure 4.9 DRIFTS spectra of CO adsorbed on Pt/A17/C30, Pt/A24/C30, Pt/A24/C30/B3 and Pt/comKL.

4.4 Catalytic Activity Measurements

As stated earlier, the aim of this work was to establish the relationship between crystal size and ethylbenzene to ortho-xylene ratio (EB/OX ratio) for n-octane aromatization. Hence, Pt/A24/C30, Pt/A17/C30 and Pt/A24/C30 with different crystal sizes were selected to study by subjecting these samples through n-octane aromatization reaction.

4.4.1 n-Octane Aromatization

The catalysts with different crystal sizes (Pt/A24/C30, Pt/A17/C30, and Pt/A24/C30/B3) were tested for n-octane aromatization reaction and compared to the Pt/comKL catalyst.

4.4.1.1 n-Octane Conversion

The resultant evaluation of conversion is shown in Figure 4.10. The conversion rapidly decreased as a function of time on stream. These results can be explained by the diffusion behavior of EB and OX. Because of their relatively large molecular size, diffusion rates through the pore zeolite of EB and OX would be slow increasing possibility of coke formation and pore plugging.

Figure 4.10 also shows that the Pt/A24/C30/B3 gave the highest conversion due to its highest Pt dispersion as reported by FTIR and hydrogen chemisorption measurements. In addition, this sample showed a higher coke formation as a result of a higher production of EB and OX than that of Pt/A24/C30 and Pt/A17/C30.

Although the Pt/comKL containing the highest Pt loading, it did not give the highest conversion due to its lowest hydrogen chemisorption. Furthermore, it generated the highest amount of coke. This outcome is in agreement with previous reports (Jongpatiwut, 2003 and Jacob, 1999). They concluded that very small Pt particles in close interaction with the zeolite walls leads to less coke formation. Consequently, between the two samples, Pt/A24/C30/B3 with higher degrees of Pt-KL zeolite interaction showed lesser coke formation.
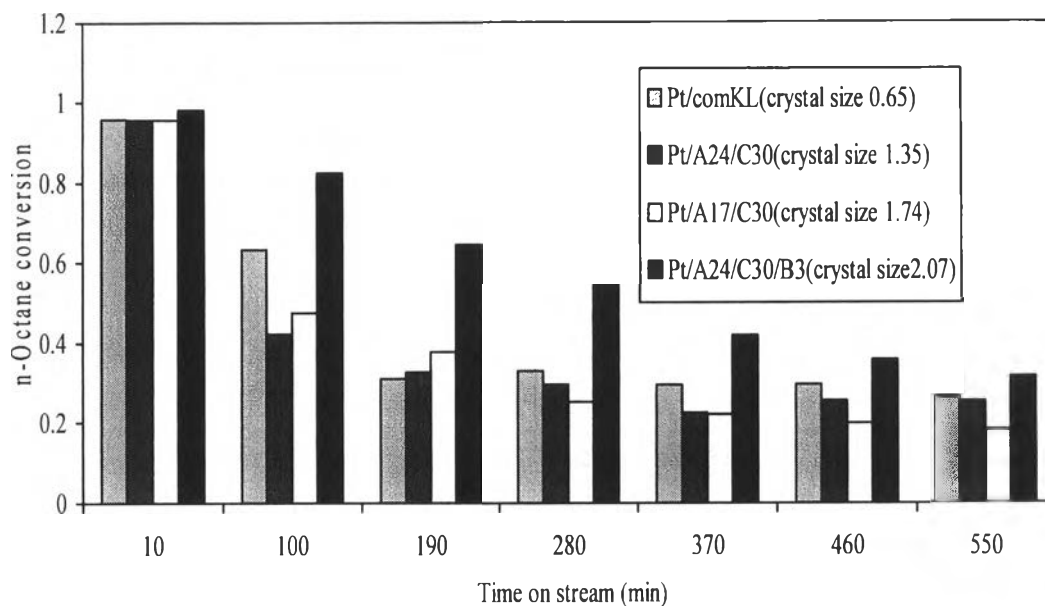
Figure 4.10 n-Octane conversion as a function of time on stream over Pt/A17/C30, Pt/A24/C30, Pt/A24/C30/B3 and Pt/comKL.

4.4.1.2 Total Aromatic Selectivity

Figure 4.11 illustrates the total aromatic selectivity as a function of time on stream over Pt/A17/C30, Pt/A24/C30, Pt/A24/C30/B3. As can be seen, at the time on stream of 10 minutes, all of the synthesized samples showed very high and similar values of total aromatic selectivitiy but slightly decreased as a function of time on stream. Low aromatic selectivity of Pt/comKL at the time on stream of 10 minutes was a result of large ensemble of Pt atoms on zeolite surface which favored hydrogenolysis reaction to aromatization reaction. Therefore, some of n-octane underwent hydrogenolysis reaction to produce small molecule even before aromatization took place. Due to coke accumulation, this process occurred in a lesser extent after time on stream exceeded 10 minutes.
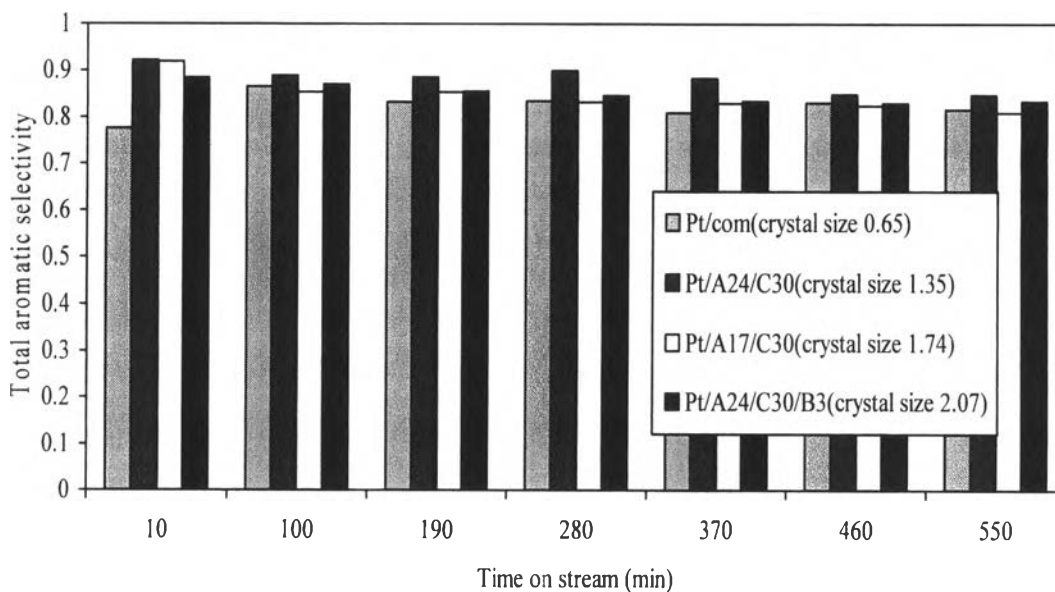
Figure 4.11 Total aromatic selectivity as a function of time on stream over Pt/A17/C30, Pt/A24/C30, Pt/A24/C30/B3 and Pt/comKL.

In terms of reaction products, benzene and toluene instead of EB and OX expected as a result of direct closure of six-membered ring was found to be major aromatic compounds. Benzene and toluene obtained from hydrogenolysis reaction and remained EB and OX were summarized in Table 4.5.

Table 4.5 Product distribution and Ethylbenzene (EB) to o-Xylene (OX) ratio over the catalysts studied at 550 min time on stream under reaction conditions: 500 ^{0}C, H_2 /n-Octane 6:1 and WHSV 5 h^{-1}

Catalyst name	Product selectivity (%)					EB/OX ratio
	Benzene	Toluene	Ethylbenzene (EB)	m- and p-Xylene	o-Xylene (OX)	
Pt/A24/C30	28.51	39.24	12.43	1.60	2.99	4.16
Pt/A17/C30	24.25	37.06	14.88	1.69	3.05	4.89
Pt/A24/C30/B3	33.25	32.92	14.06	0.70	2.39	5.88
Pt/comKL	26.64	37.17	11.59	1.69	4.53	2.56

4.4.1.3 EB/OX ratio

In the previous study (Jongpatiwut, 2003), it was found that Pt supported on commercial KL zeolite with 1 % Pt loading exhibited a higher production of EB than OX resulting in EB/OX ratio of more than 1. Because critical size diameter of OX is greater than that of EB and pore size of KL zeolite. This facilitates easy hydrogenolysis of OX to smaller molecules. They, finally, proposed that crystal size of the zeolite may have a great impact on EB/OX ratio.

Commercial KL zeolite will not be included for comparison on the effect of crystal size on EB/OX ratio. This is due to its much higher surface area and pore volume than that of synthesized KL zeolite. The first couple of samples selected for discussion were Pt/A17/C30 and Pt/A24/C30/B3. Figure 4.12 shows that EB/OX ratio obtained on both catalysts rapidly increase before stay constant. As described in previous work (Jongpatiwut, 2003), at the very first moment on stream, a higher metal particle size gave a higher EB/OX ratio. But after 550 minutes on stream, the coke deposit that partially block the pore may erase the effect of metal particle size. Therefore, different particle sizes on both catalysts did not affect on EB/OX ratio from both at several hours time on stream. As shown in Figure 4.12, Pt/A24/C30/B3 with higher crystal size gave a higher EB/OX ratio at time on stream of 550 minutes. Hence, the crystal size affected on EB/OX ratio. Moreover, the data obtained from the commercial KL zeolite in this work (bigger Pt particle size) and previous work (smaller Pt particle size (Jongpatiwut, 2003)) strongly confirmed that the effect of crystal size on EB/OX ratio is much more pronounce than that of Pt particle size. It can be explained below. Although both catalysts are different in Pt particle size, EB/OX ratio of them at time on stream of 550 minutes are similar (~ 2.5).

The second couple of samples were Pt/A24/C30 and Pt/A17/C30. Bigger crystal size of Pt/A17/C30 showed much higher EB/OX ratio although it contained smaller Pt particle size. Finally, Pt/A24/C30 and Pt/A24/C30/B3 were selected to investigate the effect of crystal size on EB/OX ratio. This result from this couple correspond with that of the second couple. Effect of the crystal size on the EB/OX ratio as indicated in linear correlation was illustrated in Figure 4.13.
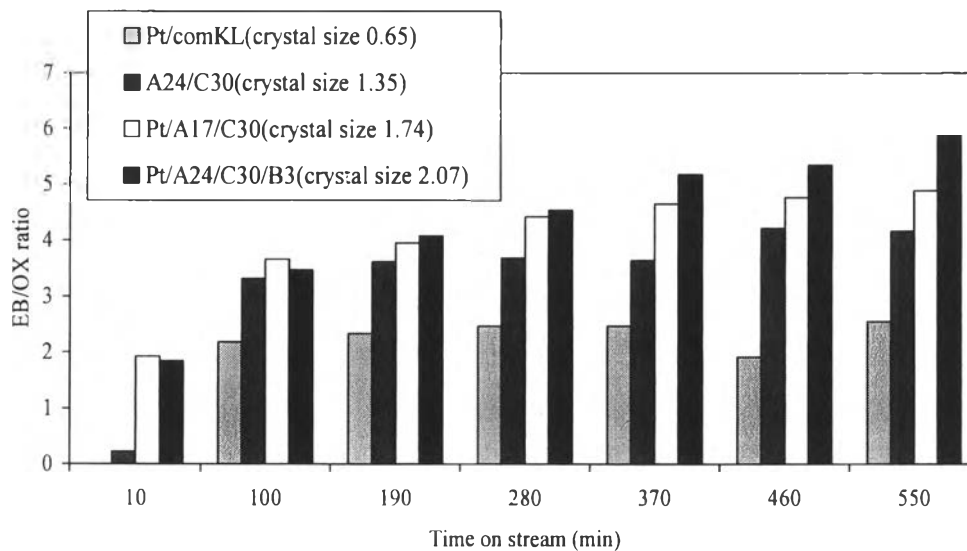
Figure 4.12   EB/OX ratio as a function of time on stream over Pt/A17/C30, Pt/A24/C30, Pt/A24/C30/B3 and Pt/comKL with different crystal sizes.
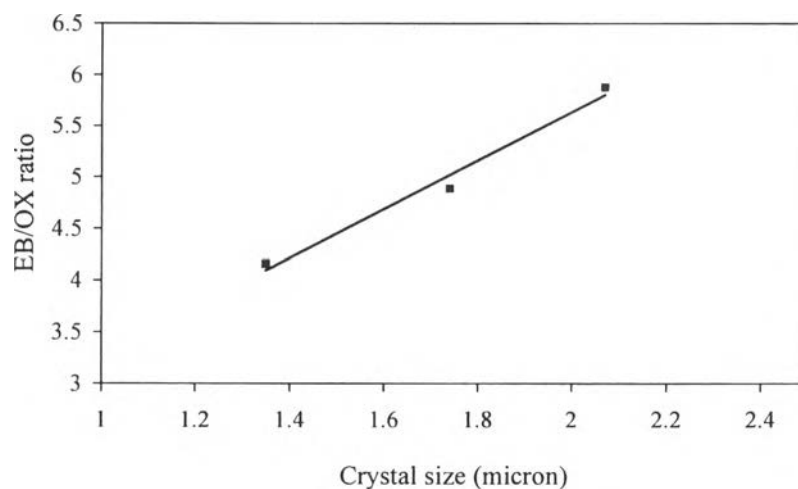

Figure 4.13 EB/OX ratio at time on stream of 550 minutes as a function of crystal size.

4.4.2 n-Hexane Aromatization

All catalysts were also tested catalytic activity with n-hexane aromatization. Contrast with n-octane aromatization, these catalysts did not exhibit significant differences in their activation patterns for n-hexane aromatization. Figures 4.14 and 4.15 show variations of conversion and benzene selectivity as a function of time on stream over Pt/A17/C30, Pt/A24/C30, Pt/A24/C30/B3, and Pt/comKL. It is clear that the conversion and benzene selectivity for commercial KL zeolite was very high and similar to that of the synthesized KL zeolite. Because of a smaller molecular size, benzene produced from n-hexane aromatization reaction could diffuse much faster than EB and OX produced from n-octane aromatization.

Moreover, These results show that all samples maintained very high performance on catalytic activity even a long time on stream of 21 hours. And these values are even comparable to that of commercial KL zeolite.
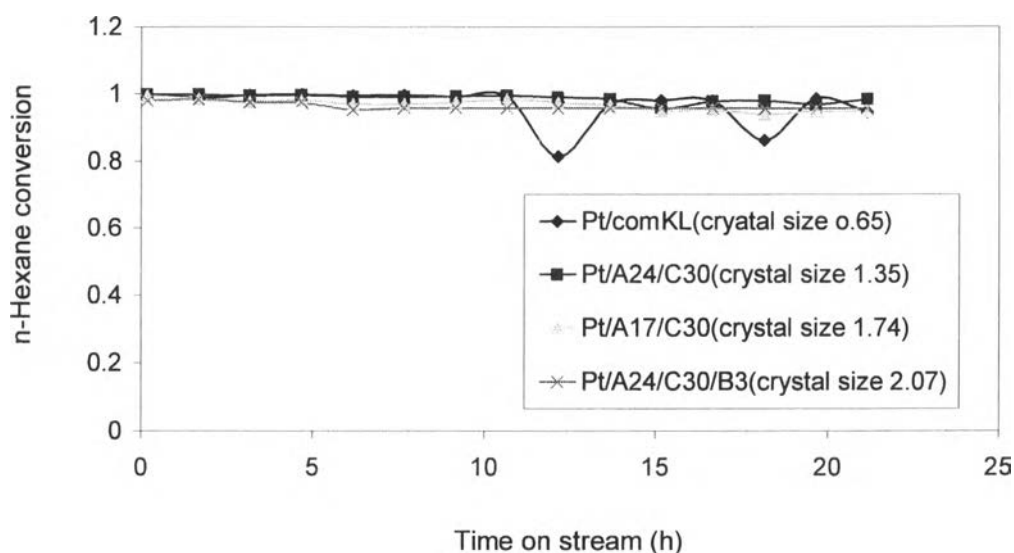

Figure 4.14 n-Hexane conversion as a function of time on stream over Pt/A17/C30, Pt/A24/C30, Pt/A24/C30/B3 and Pt/com KL.
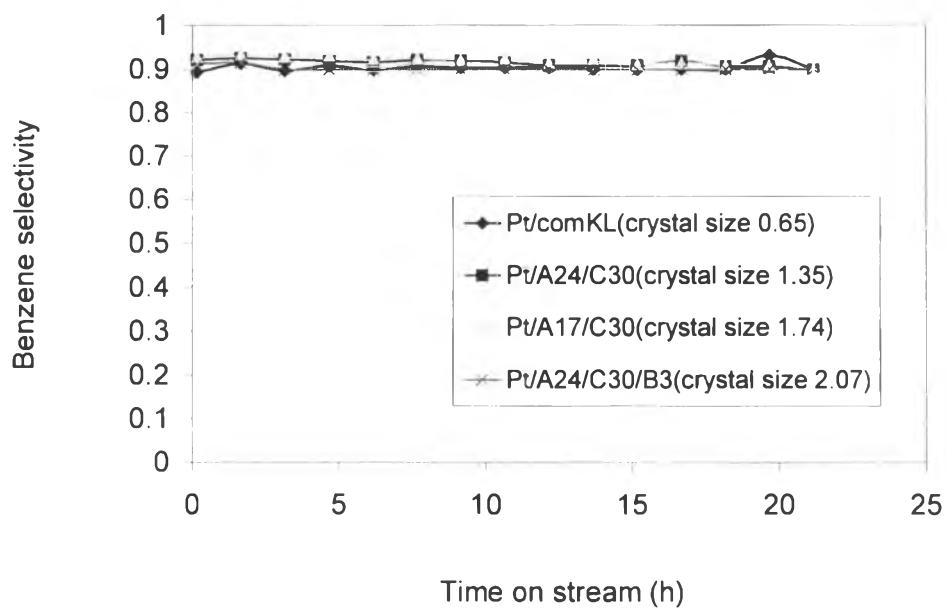
Figure 4.15 Benzene selectivity as a function of time on stream over Pt/A17/C30, Pt/A24/C30. Pt/A24/C30/B3 and Pt/comKL.